THE ASTROPHYSICAL JOURNAL, 606:L159–L162, 2004 May 10

DENSITIES AND VELOCITIES IN FAST CORONAL MASS EJECTIONS: RADIATIVE PUMPING OF THE O VI DOUBLET

J. C. RAYMOND
Harvard-Smithsonian Center for Astrophysics, 60 Garden Street, Cambridge, MA 02138; jraymond@cfa.harvard.edu
AND
A. CIARAVELLA
INAF–Osservatorio Astronomico di Palermo, Piazza del Parlamento 1, I-90134 Palermo, Italy; ciarave@oapa.astropa.unipa.it
Received 2003 December 5; accepted 2004 March 29; published 2004 April 15

ABSTRACT

In very fast coronal mass ejections (CMEs), it is possible for O VI ions to scatter Lyβ photons that originate in the solar chromosphere and for the λ1037 transition of O VI to scatter λ1032 photons from the solar transition region. This scattering process can be identified by departures of the O VI I_{1032}/I_{1037} intensity ratio from its collisional value of 2. We report the first detection of this effect in a CME that occurred on 2000 June 28, and we show that this pumping provides a density diagnostic for CMEs faster than 1600 km s^{-1}. At heliocentric distances near 3 $R_\odot$, this diagnostic is useful for densities in the 5×10^5–10^7 cm^{-3} range.

Subject headings: Sun: activity — Sun: coronal mass ejections (CMEs)

1. INTRODUCTION

Coronal mass ejections (CMEs) are generally observed by white-light coronagraphs. A series of coronagraph images yields the CME mass, velocity, and acceleration in the plane of the sky, and the morphology as projected onto the plane of the sky (e.g., Vourlidas et al. 2000; St. Cyr et al. 1999; Sheeley et al. 1999). Spectroscopic observations complement these images by measuring the line-of-sight component of velocity, providing insights into the three-dimensional morphology (Ciaravella et al. 2000), the composition and ionization state (Ciaravella et al. 1997; Ko et al. 2003), and electron and ion temperatures (Raymond et al. 2000; Innes et al. 2001; Ciaravella et al. 2001). Spectroscopic observations can also be used to determine the plasma density, which, in combination with composition, ionization state, and temperature, can be used to constrain the thermal history of the ejected plasma and therefore the heating and cooling rates to which it has been subjected (Akmal et al. 2001; Ciaravella et al. 2001). The density is also useful for disentangling the internal structure of the CME and for direct comparison with numerical simulations (e.g., Amari et al. 1999; Roussev et al. 2003).

In a few cases, classical density-sensitive line ratios such as [O V] λ1213/O V] λ1218 can be used to obtain the density (Akmal et al. 2001). More frequently, however, no line pairs are available that have a critical density close to the density of the observed plasma. Fortunately another class of density diagnostics is available. Several of the brightest lines, the O VI doublet λλ1032, 1037 and the lower Lyman lines of hydrogen, are formed by both collisional excitation and radiative scattering. As the former scales as ion density times electron density, while the latter is proportional to ion density alone, the ratio is proportional to electron density. The radiative scattering term depends on resonance between the scattering ions and the solar emission line that pumps them, so it depends on the speed of the plasma with respect to the Sun. Thus, diagnostics for both outflow speed and density are possible using Lyα (Withbroe et al. 1982) and the O VI doublet (Noci, Kohl, & Withbroe 1987), and they have been widely exploited in the analysis of spectra from the Ultraviolet Coronagraph Spectrometer (UVCS) aboard the *Solar and Heliospheric Observatory* (Kohl et al. 1995, 1997). A particularly useful pumping of the O VI λ1037 line by the C II λλ1036.3, 1037.0 doublet at velocities of 172 and 371 km s^{-1} permits diagnostics near these speeds (Li et al. 1998). Examples of this technique include outflow speeds in coronal holes (Cranmer et al. 1999), streamers (Strachan et al. 2002), and CMEs (Akmal et al. 2001; Ciaravella et al. 1999) and densities in streamers (Ko et al. 2002; Parenti et al. 2000)

Here we discuss a diagnostic appropriate to fast CMEs, the pumping of O VI λ1037.61 by O VI λ1031.91 (1650 km s^{-1}), the pumping of O VI λ1031.91 by Lyβ (1810 km s^{-1}), as well as the pumping of Lyα by Si III λ1206.51 (2280 km s^{-1}). This pumping is the most directly detectable in the O VI doublet because any departures from a 2 : 1 intensity ratio of the collisional components must be due to radiative pumping. The technique is only useful for fast CMEs above 1600 km s^{-1}, but these are among the most powerful and interesting cases. We present the formulae to convert a measured O VI doublet ratio to a density, and we apply the diagnostic to a fast CME observed on 2000 June 28, which we believe is the first reported instance of this pumping.

2. THEORY

When the outflow speed is as high as 1800 km s^{-1}, the pumping of O VI λ1032 by Lyβ occurs, and the O VI λ1032/λ1037 line ratio is greater than 2. In this case, the plasma density is

$$n_e = \frac{\sigma_{1032} I_{\rm disk}({\rm Ly}\beta) W}{q_{1032}} \frac{I_{\rm coll}(1032)}{I_{\rm rad}(1032)}, \quad (1)$$

where σ_{1032} is the effective scattering cross section (oscillator strength from Verner, Verner, & Ferland 1996) and W is the dilution factor $2\pi\,[1 - (1 - 1/r^2)^{1/2}]$, with the distance from Sun center r in solar radii. $I_{\rm coll}$ and $I_{\rm rad}$ are the collisionally excited and radiatively excited components of the λ1032 intensity, respectively, and the total intensity, $I(1032)$, is their sum. The collisional excitation rate coefficient for the 1032 Å line is q_{1032} (CHIANTI; Young et al. 2003). Similarly, when the ob-

served ratio is less than 2 and the pumping of O VI λ1037 by O VI λ1032 dominates,

$$n_e = \frac{\sigma_{1037} I_{\rm disk}(1032) W}{q_{1037}} \frac{I_{\rm coll}(1037)}{I_{\rm rad}(1037)}. \quad (2)$$

By simple algebra, the ratios of collisional to radiative components of the λ1032 line can be obtained from the O VI λ1032/λ1037 doublet ratio R:

$$n_e = \frac{\sigma_{1032} I_{\rm disk}({\rm Ly}\beta) W}{q_{1032}} \frac{2}{R-2} \quad ({\rm for}\ R > 2), \quad (3)$$

$$n_e = \frac{\sigma_{1037} I_{\rm disk}(1032) W}{q_{1037}} \frac{2-R}{2R} \quad ({\rm for}\ R < 2). \quad (4)$$

The effective scattering cross section σ_{1032} depends on the effective velocity width of the scattering ion line profile. At a heliocentric distance r, the solar disk subtends angles out to $\theta = \arcsin(1/r)$, and the velocity component away from the solar limb is $V\cos(\theta)$. Thus, pumping will occur at speeds between V and $V\sec\theta$.

Pumping of Lyα by Si III may also be significant, but it is more difficult to use as a diagnostic. In coronal streamers, it is easy to separate the collisional and radiative components because the collisional Lyα-to-Lyβ intensity ratio is insensitive to temperature in 1×10^6 K gas. However, at the lower temperatures found in CMEs, the ratio is quite sensitive to temperature. In principle, the intensities of several Lyman lines could be used to separate temperature and the collisional-to-radiative ratio, but this would be subject to rapidly accumulating uncertainties. It might be possible, however, to identify anomalous peaks in the Lyα-to-Lyβ ratio in the time history of a CME and to use them to pick out times when the outflow speed is near the resonant value.

3. APPLICATION

Using UVCS, a fast CME was observed on 2000 June 28 and described by Ciaravella et al. (2004), with emphasis on the manifestations of shock waves. Here we consider the bright strands of relatively low ionization plasma, presumably the ejected prominence, that lay inside the CME. At a projected heliocentric distance of 2.35 $R_\odot$, appropriate for the 2000 June 28 event, the solar disk subtends angles out to $\theta = 25°$. The observed plasma is not in the plane of the sky, however, and based on the Doppler shifts, Ciaravella et al. (2004) estimate an average angle with the plane of the sky of ~38°, or an actual distance of 3 $R_\odot$. At this heliocentric distance, the solar disk subtends angles up to 20°. The velocity component away from the solar limb is $V\cos 20° = 0.94V$, so pumping will occur in O VI λ1037 at speeds between 1650 and 1755 km s^{-1} and for O VI λ1032 at speeds between 1810 and 1925 km s^{-1}. This implies velocity widths of 110 km s^{-1} for the scattering ions. Based on the widths of the narrower components of the Lyα line, the plasma temperature is about 3.5×10^5 K. The dilution factor at 3 $R_\odot$ is 0.36. The solar disk intensities of O VI λ1032 and Lyβ are 1.94×10^{13} and 4.13×10^{13} photons cm^{-2} s^{-1} sr^{-1}, respectively, at solar minimum (Raymond et al. 1997), and these should be multiplied by factors of about 1.8 at solar maximum (e.g., Rottman et al. 2001).

Thus, for a heliocentric distance of 3 $R_\odot$ and solar maximum conditions,

$$n_e = 3.3 \times 10^6 \frac{2}{R-2}\ {\rm cm}^{-3} \quad (R > 2), \quad (5)$$

$$n_e = 1.6 \times 10^6 \frac{R}{2-R}\ {\rm cm}^{-3} \quad (R < 2). \quad (6)$$

Figure 1 shows the O VI λ1032 and O VI λ1037 intensities as functions of distance along the UVCS slit (*horizontal axis*) and time (*vertical axis*). To the extent that the CME maintained a constant shape and moved perpendicular to the axis, this would be an image of the CME if the vertical pixels were scaled to the CME speed times the exposure time. The aspect ratio would be correct for a speed of 150 km s^{-1}. The velocity actually declines with time from over 1000 km s^{-1} for the first material to reach the slit to about 50 km s^{-1} for the last material at the bottom of the image (Ciaravella et al. 2004).

The left panel of Figure 2 shows the intensity ratio $I(1032)/I(1037)$. We have binned the data by two spatial bins (to 42″) and two exposures (to 240 s) in order to improve the statistical accuracy. For each spatial position in each exposure, if the ratio did not differ from 2.0 by more than 2 σ, R was set to 2.0, so that only statistically significant departures from the collisional ratio appear as light ($R < 2$) or dark gray ($R > 2$) pixels. The middle panel indicates the dominant pumping mechanism, which we identify on the basis of line ratio and total velocity. We estimate the total outflow speed by adding in quadrature the Doppler speed and the speed in the plane of the sky. We measure the Doppler shift of the brightest intensity peak, and we estimate the speed in the plane of the sky by dividing the distance between each position of a pixel on the UVCS slit (Δx) and the top of the expanding loop in the EUV Imaging Telescope image at 18:48 UT by the time difference between the exposure and 18:48 UT (Δt), giving a two-dimensional velocity map. This speed is probably an underestimate for most pixels because the loop was probably still accelerating during this time interval. Because this is a minimum speed, we can be confident that speeds above 400 km s^{-1} preclude pumping by C II (Li et al.1998). Thus, we identify pixels with $R > 2$ and $V > 400$ km s^{-1} as Lyβ pumping of the 1032 Å line (*dark blue*), $R < 2$ and $V > 400$ km s^{-1} as O VI λ1032 pumping of the 1037 Å line (*light blue*), $R < 2$ and $V < 400$ km s^{-1} as C II pumping of the 1037 Å line (*red*), and $R > 2$ and $V < 200$ km s^{-1} as O VI λ1032 pumping by the chromospheric 1032 Å line (*orange*).

The right panel in Figure 2 shows the densities derived for those pixels. Densities range from 1.3×10^6 to 4×10^7 cm^{-3}. Higher densities would produce O VI ratios close to 2 and would therefore be difficult to measure. Ratios near 2 will also occur where the outflow speed is outside the ranges of resonance; 172–183 and 371–395 km s^{-1} for C II pumping, and 1660–1910 km s^{-1} for pumping by O VI λ1032 or Lyβ. However, the bright pixels encompass much of the brightest O VI emission, so the derived densities are probably at the upper end of the density range.

The density and the brightness can be combined to determine the thickness of the emitting region along the line of sight:

$$l = 4\pi I_{\rm coll}(1032)/(n_e^2 q_{1032} {\rm AB_O}\, f_{\rm O\,VI}). \quad (7)$$

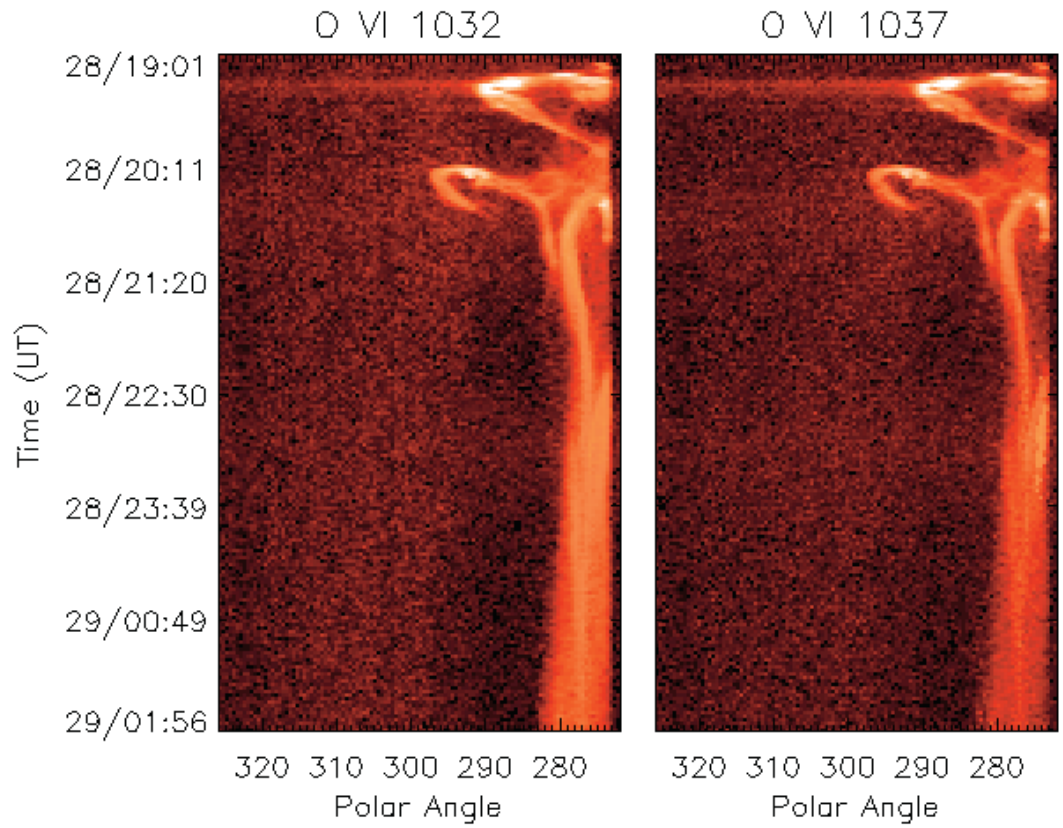

FIG. 1.—Intensities of the O VI λ1032 and λ1037 lines as functions of time (*vertical axis*) and distance along the slit (*horizontal axis*)

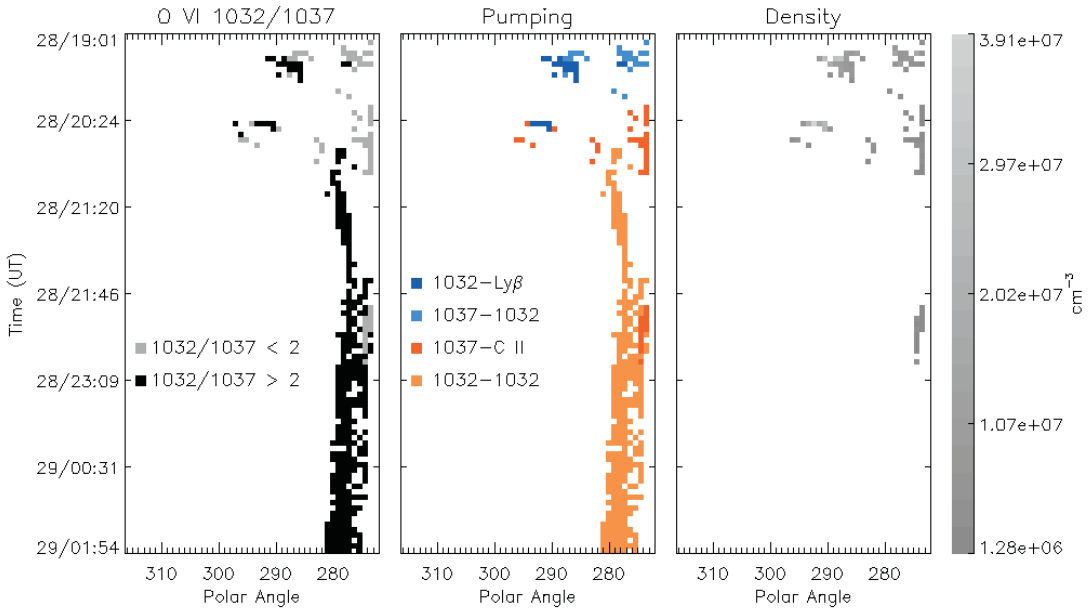

FIG. 2.—Intensity ratio of the O VI λ1032 and λ1037 lines (*left panel*), dominant pumping transition (*middle panel*; see text), and derived density (*right panel*)

Assuming a photospheric abundance for AB_O of 8.74 (Allende Prieto, Lambert, & Asplund 2002), and ionization fraction and excitation rates at 3×10^5 K from CHIANTI (Young et al. 2003), we estimate a thickness of about 0.1–0.2 $R_\odot$, or about the widths of the bright strands along the UVCS slit. Thus, we infer that the bright strands are narrow threads rather than tangencies of an emitting sheet to the line of sight. The assumption of ionization equilibrium is questionable (Akmal et al. 2001; Ciaravella et al. 2001), but the relative strengths of O v] λ1218 and the O vi lines are consistent with this assumption (Ciaravella et al. 2004).

4. DISCUSSION

We have presented evidence for radiative pumping of the O vi lines in the high-speed ejecta of a CME on 2000 June 28, and we have developed a diagnostic for the electron densities in fast CMEs. While it can only be applied to gas in specific velocity ranges, the fastest CME material generally reaches the UVCS slit first, and the velocity of the trailing material gradually declines. Thus, CMEs faster than 2000 km s^{-1} are likely to have some regions where resonant pumping occurs and for which the density can be inferred. These densities are especially useful for determining the energy budget and heating of the CME plasma (Akmal et al. 2001; Ciaravella et al. 2001), and they can be compared with numerical simulations.

The method should be fairly robust, but there are a few caveats. First, the flux of illuminating line emission from the Sun can be significantly enhanced for a few minutes very early in the flare (Raymond et al. 2003), which would lead to an underestimate of the density. Second, material at different speeds could coexist along the line of sight. In the worst case, both plasma in between 1660 and 1770 km s^{-1} and plasma between 1800 and 1910 km s^{-1} would contribute, yielding an O vi ratio closer to 2 and an overestimate of the density. At heliocentric distances below 3 $R_\odot$, the projection angle for illumination from the solar limb is more severe, leading in principle to overlapping velocity ranges for the two pumping processes. A third potential source of error is the collisional excitation rate, which depends on the electron temperature. In some cases, a temperature diagnostic is available (e.g., Ciaravella et al 2000), but if one assumes $T_e = 3 \times 10^5$ K when the actual temperature is $T_e = 5 \times 10^4$ K, one underestimates the collisional excitation rate, and therefore the density, by an order of magnitude.

This work was supported by NASA grant NAG5-12827 to the Smithsonian Astrophysical Observatory.

REFERENCES

Akmal, A., Raymond, J. C., Vourlidas, A., Thompson, B., Ciaravella, A., Ko, Y.-K., Uzzo, M., & Wu, R. 2001, ApJ, 553, 922
Allende Prieto, C., Lambert, D. L., & Asplund, M. 2002, ApJ, 573, L137
Amari, T., Luciani, J. F., Mikić, Z., & Linker, J. 1999, ApJ, 518, L57
Ciaravella, A., et al. 1997, ApJ, 491, L59
———. 1999, ApJ, 510, 1053
———. 2000, ApJ, 529, 575
Ciaravella, A., Raymond, J. C., Reale, F., Strachan, L., & Peres, G. 2001, ApJ, 557, 351
Ciaravella, A., Raymond, J. C., Kahler, S., Vourlidas, A., & Li, J. 2004, ApJ, submitted
Cranmer, S. R., et al. 1999, ApJ, 511, 481
Innes, D. E., Curdt, W., Schwenn, R., Solanki, S., Stenborg, G., & McKenzie, D. E. 2001, ApJ, 549, L249
Ko, Y.-K., Raymond, J. C., Li, J., Ciaravella, A., Michels, J., Fineschi, S., & Wu, R. 2002, ApJ, 578, 979
Ko, Y.-K., Raymond, J. C., Lin, J., Lawrence, G., Li, J., & Fludra, A. 2003, ApJ, 594, 1068
Kohl, J. L., et al. 1995, Sol. Phys., 162, 313
———. 1997, Sol. Phys., 175, 613
Li, X., Habbal, S. R., Kohl, J., & Noci, G. 1998, ApJ, 501, L133
Noci, G., Kohl, J. L., & Withbroe, G. L. 1987, ApJ, 315, 706
Parenti, S., Bromage, B. J. I., Poletto, G., Noci, G., Raymond, J. C., & Bromage, G. E. 2000, A&A, 363, 800
Raymond, J. C., Ciaravella, A., Dobrzycka, D., Strachan, L., Ko, Y.-K., Uzzo, M., & Raouafi, N.-E. 2003, ApJ, 597, 1106
Raymond, J. C., et al. 1997, Sol. Phys., 175, 645
———. 2000, Geophys. Res. Lett., 27, 1439
Rottman, G., Woods, T., Snow, M., & DeToma, G. 2001, Adv. Space Res., 27, 1927
Roussev, I. I., Forbes, T. G., Gombosi, T. I., Sokolov, I. V., DeZeeuw, D. L., & Birn, J. 2003, ApJ, 588, L45
Sheeley, N. R., Jr., Walters, J. H., Wang, Y.-M., & Howard, R. A. 1999, J. Geophys. Res., 104, 24739
St. Cyr, O. C., Burkepile, J. T., Hundhausen, A. J., & Lecinski, A. R. 1999, J. Geophys. Res., 104, 12493
Strachan, L., Suleiman, R., Panasyuk, A. V., Biesecker, D. A., & Kohl, J. L. 2002, ApJ, 571, 1008
Verner, D. A., Verner, E. M., & Ferland, G. J. 1996, At. Data Nucl. Data Tables, 64, 1
Vourlidas, A., Subramanian, P., Dere, K. P., & Howard, R. A. 2000, ApJ, 534, 456
Withbroe, G. L., Kohl, J. L., Weiser, H., & Munro, R. H. 1982, Space Sci. Rev., 33, 17
Young, P. R., Del Zanna, G., Landi, E., Mason, H. E., & Landini, M. 2003, ApJS, 144, 135